Computational Thermal Sciences, 3 (2): xxx–xxx (2011)

PARAMETRIC STUDY OF THE PRESSURE CHARACTERISTIC CURVE IN A BOILING CHANNEL

E. Manavela Chiapero, M. Fernandino, & C. A. Dorao*

Department of Energy and Process Engineering, Norwegian University of Science and Technology, Trondheim, Norway

*Address all correspondence to M. Fernandino E-mail: maria.fernandino@ntnu.no.

The main objective of this work is to understand the behavior of the pressure drop of a boiling fluid along a heated pipe as a function of the mass flux. The steady-state plot of the pressure drop against the mass flux of a heated boiling channel with subcooled liquid at the inlet is widely used for pressure drop and thermal oscillations simulations. The influence of several important parameters, such as the heat applied, the inlet pressure, and the inlet temperature, is analyzed. As the inlet pressure goes down, the steepness of the negative slope of the static curve increases. The inlet temperature has a very important role in this plot, showing that the negative slope of the curve gets steeper as the subcooling increases. Although the amount of heat applied to the test section is found to have no influence on the shape of the static curve, the axial distribution of the heat along the heated section plays a very important role in the steepness of the negative slope of the steady-state pressure drop versus mass flux plot.

KEY WORDS: *horizontal pipe, numerical simulation, two-phase, N-shape, Ledinegg, instability, heat distribution*

1. INTRODUCTION

Two-phase flow in boiling channels is a widely studied subject because of its major role in nuclear reactors safety, heat exchangers performance, and cryogenic processes. The possible occurrence of flow instabilities is undesirable because they cause mechanical vibrations, problems of system control, and in extreme circumstances, disturb the heat transfer characteristics so that the heat transfer surface may burn out. Under certain circumstances, failure could be produced due to thermal fatigue resulting from continuous cycling of the wall temperature.

The instabilities observed in the above-mentioned processes can be classified as static (eg., Ledinegg instability) or dynamic. Ledinegg instability is characterized by a sudden change in the mass flow rate. Dynamic instabilities can be characterized as density-wave-type oscillations, pressure-drop-type oscillations, acoustic oscillations, and thermal oscillations. Boure et al. (1973) made a wide clasiffication and description of the different types of two-phase flow instabilities. Pressure-drop oscillations are closely connected with the thermohydraulic steady-state behavior of a heated pipe. This behavior is usually represented by the total pressure-drop along the pipe versus the mass flux. For a boiling channel with subcooled liquid at the inlet, this curve can show a negative slope region. Liu et al. (1995) used this plot to formulate a planar system for pressure drop oscillations in a single-channel boiling system in order to provide the whole bifurcation diagram of the dynamic system. Because the periods of the pressure-drop oscillations are very large compared to the residence time of a fluid particle through the system, quasi steady-state conditions can be assumed along the heated section [Gurgenci et al. (1983); Kakac et al. (1990)]. Kakac and Cao (2009) analyzed pressure drop oscillations and the thermal oscillations induced by the previous ones in vertical and horizontal systems using the steady-state pressure drop versus mass flux plot.

Boure et al. (1973) analyzed the effect of pressure, inlet subcooling, mass flow rate, and power on density-wave oscillations. More recently, Kakac and Bon (2008) summarized the effects, observed during experiments, of inlet subcooling, heat flux, and flow rate on the system stability. Farhadi (2009) developed a simple static model for the

1940–2503/11/$35.00

NOMENCLATURE

A	area [m^2]
Bo	Boiling number
c_p	specific heat at constant pressure [J/kg K]
D_i	inner diameter [m]
D_o	outer diameter [m]
e	specific energy [J/kg]
f	friction factor
f_{Dc}	Darcy friction factor
Fr	Froude number
g	gravitational acceleration [m/s^2]
G	mass flux [kg/m^2s]
h	heat transfer coefficient [W/m^2 K]
H_{lv}	specific enthalpy of vaporization [J/kg]
k	thermal conductivity [W/m K]
L	total tube length [m]
Nu	Nusselt number
P	pressure [Pa]
Per	heated perimeter [m]
Pr	Prandtl number
q	heat flux [W/m^2]
Re	Reynolds number
T	temperature [K]
V	velocity [m/s]
We	Weber number
x	thermodynamic quality
z	axial coordinate along the pipe [m]

Greek symbols

α	void fraction
ϵ	tube roughness [m]
μ	viscosity [Pa s]
ρ	density [kg/m^3]
σ	surface tension [N/m]
τ	shear stress [N/m^2]
ϕ	two-phase multiplier

Subscripts

l_0	total mass flux flowing with the liquid properties
l	liquid
out	outlet of the pipe
sub	subcooling
tp	two-phase
v_0	total mass flux flowing with the vapor properties
v	vapor
w	pipe wall

prediction of Ledinegg-type instability based on the negative slope of the pressure drop versus the mass flow rate plot and its dependence on the inlet temperature, exit pressure, and surface heat flux among other parameters. In this work, we are interested in the total presure drop along the heated section versus the mass flux curve. This behavior is a determinant factor for the ocurrence of pressure-drop oscillations and Ledinegg-type instabilities. These dynamic and static instabilities need, in order to be produced, together with other factors, a negative slope in the plot of the pressure drop against the mass flow rate. The main objective of the work is then to analyze and understand this behavior and the main parameters that play an important role in the shape of this plot.

In Section 2, the model proposed for describing the heated pipe is presented. Section 3 describes the simulation approach. In Section 4, the solution algorithm is described. Section 5 presents the necessary condition for the ocurrence of the negative slope. Section 6 shows the parameter sensitivity analysis and its discussion. Finally, Section 7 presents the main conclusions drawn from this work.

2. PROBLEM DESCRIPTION

The present model describes the behavior of a refrigerant flowing in a heated pipe. The model is a steady-state 1D model. The fluid enters the pipe as subcooled liquid, and, depending on the heat applied to the pipe, can leave the heated section as liquid, vapor and liquid two-phase flow, or superheated vapor. The main assumptions for the modeling of the two-phase region of the pipe are that liquid and vapor are at the same pressure and in thermodynamic equilibrium. The fluid used for the simulations is

the refrigerant R134a because it is a widely used refrigerant these days and there is a lot of information available about its thermal-hydraulic behavior. The dimensions of the tube were selected in order to be similar to the sizes of a compact heat exchanger. The heated section is 1 m long. The inner diameter is 5 mm, and the thickness of the wall is 1.5 mm.

2.1 Conservation Equations

The model solves the conservation of mass, momentum, and energy equations for the subcooled liquid at the inlet, the two-phase flow along the pipe, and the superheated vapor (if any) at the outlet.

2.1.1 Single-Phase Flow (Subcooled Liquid, Superheated Vapor)

The conservation of the mass equation for the single phase regions can be written as follows:

$$\frac{\partial}{\partial z}\left(\rho_j V_j\right) = 0 \tag{1}$$

where the suffix j stands for the phase (l for the subcooled liquid region or v for the superheated vapor region), ρ_j [kg/m^3] is the density of the j phase, V_j [m/s] stands for the Eulerian area averaged value of the velocity over the cross section of the duct of the j phase and z [m] is the axial direction.

For the conservation of momentum equation, we have

$$\rho_j V_j \frac{\partial V_j}{\partial z} = -\frac{\partial P}{\partial z} - \frac{4}{D_\mathrm{i}}\tau_\mathrm{w}, \tag{2}$$

where P is the pressure, D_i the inner diameter and τ_w the wall shear stress.

Finally, the conservation of energy equation for the single-phase regions is

$$\rho_j V_j \frac{\partial e_j}{\partial z} = \frac{4}{D_\mathrm{i}} q_\mathrm{w} \tag{3}$$

where e_j is the Eulerian area averaged value of the specific energy over the cross section of the pipe of the j phase and q_w stands for the heat flux applied to the wall.

2.1.2 Two-Phase Flow

The model for the two-phase flow region is a simplification of the two-phase separated flow model presented by Sripattrapan and Wongwises (2005). Although their model contains an energy equation, allowing for different temperatures for each phase and heat exchange between them, in our simplified model the two phases are considered at thermodynamic equilibrium.

The conservation of mass for the liquid phase can be expressed as

$$\frac{\partial}{\partial z}\left[(1-\alpha)\,\rho_\mathrm{l} V_\mathrm{l}\right] = -\frac{4}{D_\mathrm{i}}\frac{q_\mathrm{w}}{H_\mathrm{lv}} \tag{4}$$

where α is the cross-sectional void fraction and H_lv is the specific enthalpy of vaporization.

The conservation of mass for the vapor phase is then

$$\frac{\partial}{\partial z}\left(\alpha\rho_\mathrm{v} V_\mathrm{v}\right) = \frac{4}{D_\mathrm{i}}\frac{q_\mathrm{w}}{H_\mathrm{lv}} \tag{5}$$

The momentum equation for both phases together is

$$\frac{\partial}{\partial z}\left[(1-\alpha)\rho_\mathrm{l} V_\mathrm{l}^2\right] + \frac{\partial}{\partial z}\left(\alpha\rho_\mathrm{v} V_\mathrm{v}^2\right) = -\frac{\partial P}{\partial z} - \frac{4}{D_\mathrm{i}}\tau_\mathrm{w} \tag{6}$$

The boundary conditions for the problem are the inlet pressure, inlet temperature, and mass flux.

Because heat is applied to the fluid, the liquid can start boiling in some part of the pipe and, in some other part, can also evaporate completely and become superheated vapor. For this reason, the pipe will be split into several parts. At the beginning, we will always have single-phase fluid, as long as the fluid has a positive subcooling temperature. After that, if the heat load is large enough, or the mass flux small enough, the fluid will start boiling, leading to a two-phase zone. If the fluid boils completely before it reaches the end of the pipe, then the superheated vapor regions begins leading to a new single-phase region. The three possible scenarios with subcooled liquid at the inlet are shown in Fig. 1.

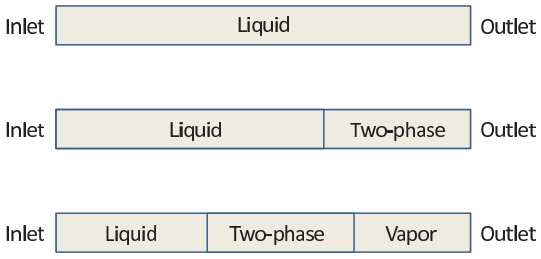

FIG. 1: Length of single phase liquid flow, two-phase flow, and single-phase vapor flow regions, along the pipe for three different cases.

First, we can calculate the liquid flow region length from the beginning of the pipe until boiling starts with the following equation:

$$L_{\mathrm{l}} = \frac{G}{q_{\mathrm{w}}} \frac{D_{\mathrm{i}}^2}{4D_{\mathrm{o}}} c_{\mathrm{pl}} T_{\mathrm{sub}} \tag{7}$$

where L_{l} is length needed in order to set the refrigerant to saturated conditions, G is the total mass flux (i.e., the product of the cross section area averaged values of the density and the velocity), D_{o} is the outer diameter of the heated pipe, c_{pl} is the specific heat at constant pressure of the liquid phase and T_{sub} is the subcooling temperature.

If this length is larger than the pipe length, then the liquid region length is the total length of the pipe. However, if it is smaller than the length of the pipe, we can have a two-phase flow region or a two-phase region plus a single-phase vapor region. The two-phase flow region length can be calculated as follows:

$$L_{\mathrm{tp}} = \frac{G}{q_{\mathrm{w}}} \frac{D_{\mathrm{i}}^2}{4D_{\mathrm{o}}} H_{\mathrm{lv}} \tag{8}$$

where L_{tp} is length needed to evaporate the whole refrigerant flow.

Finally, if the sum of the single phase region length and the two-phase flow length is less than the total length of the pipe, the length of the vapor zone will be

$$L_{\mathrm{v}} = L - L_{\mathrm{l}} - L_{\mathrm{tp}}, \tag{9}$$

where L_{v} is the vapor region length and L is the total heated section length.

The boundary conditions for the solution of the two-phase region are the mass flux, pressure, and thermodynamic quality at the inlet (taken from the solution at the end of the liquid region). For the vapor single-phase region, the boundary conditions are the mass flux, pressure, and temperature at the inlet (taken from the solution at the end of the two-phase region).

2.2 Closure Relations

The equations needed for the closure of the system are listed below. For the frictional pressure drop, single-phase friction factor is given by Haaland (1983),

$$\frac{1}{\sqrt{f_{\mathrm{Dc}}}} = -1.8 \log \left[\frac{6.9}{\mathrm{Re}} + \left(\frac{\epsilon / D_{\mathrm{i}}}{3.7} \right)^{1.11} \right]$$

where f_{Dc} is the Darcy friction factor, Re is the Reynolds number, and $\epsilon / D_{\mathrm{i}}$ is the relative roughness.

For the two-phase frictional pressure drop term in Eq. (6),

$$\tau_{\mathrm{w}} = f_{\mathrm{l0}} \frac{G^2}{2\rho_{\mathrm{l}}} \phi_{\mathrm{l0}}^2,$$

where ϕ_{l0}^2 is the Friedel two-phase multiplier (Whalley (1987)),

$$\phi_{l0}^2 = E + \frac{3.24 M H}{\mathrm{Fr}^{0.045} \mathrm{We}^{0.035}}$$

where

$$M = x^{0.78} \left(1 - x\right)^{0.224}$$

$$E = \left(1 - x\right)^2 + x^2 \frac{\rho_{\mathrm{l}} f_{\mathrm{v0}}}{\rho_{\mathrm{v}} f_{\mathrm{l0}}},$$

$$\mathrm{We} = \frac{G^2 D_{\mathrm{i}}}{\rho_h \sigma},$$

$$\mathrm{Fr} = \frac{G^2}{g D_{\mathrm{i}} \rho_h^2},$$

$$H = \left(\frac{\rho_{\mathrm{l}}}{\rho_{\mathrm{v}}} \right)^{0.91} \left(\frac{\mu_{\mathrm{v}}}{\mu_{\mathrm{l}}} \right)^{0.19} \left(1 - \frac{\mu_{\mathrm{v}}}{\mu_{\mathrm{l}}} \right)^{0.7}$$

$$\rho_h = \frac{\rho_{\mathrm{l}} \rho_{\mathrm{v}}}{\rho_{\mathrm{l}} x + \left(1 - x\right) \rho_{\mathrm{v}}}$$

Fr is the Froude number, We is the Weber number, σ is the surface tension, and μ_L and μ_{v} are the dynamic viscosities of the liquid and the vapor phases respectively. The friction factors f_{v0} and f_{l0} are for the total mass flow as all vapor and all liquid, respectively. These friction factors are calculated from

$$f = \frac{f_{\mathrm{Dc}}}{4}$$

For the wall temperature, the single-phase heat transfer is obtained from the Dittus-Boelter correlation (Stephan, 1992),

$$\mathrm{Nu} = 0.023 \mathrm{Re}^{0.8} \mathrm{Pr}^{0.4}$$

$$h = \frac{k \mathrm{Nu}}{D_{\mathrm{i}}}$$

where Nu is the Nusselt number, Pr is the Prandtl number, k is the thermal conductivity of the given phase, and h is the heat transfer coefficient between the pipe wall and the single-phase fluid.

For the two-phase flow heat transfer, we use the Gungor and Winterton (1987) correlation based only in convective boiling

$$h_{\rm tp} = Ch,$$

$$C = 1 + 3000{\rm Bo}^{0.86} + 1.12\left(\frac{x}{1-x}\right)^{0.75}\left(\frac{\rho_{\rm l}}{\rho_{\rm v}}\right)^{0.41} \quad (10)$$

$$\text{Bo} = \frac{q_{\rm w}}{GH_{\rm lv}},$$

where h is the single-phase Dittus-Boelter heat transfer coefficient for the liquid using only the liquid fraction mass flux and Bo is the boiling number.

3. NUMERICAL RESOLUTION OF THE PROBLEM

The problem is solved using the least-squares method (Jiang, 1998). The least-squares formulation is based on the minimization of a norm–equivalent functional. For simplicity, the system of equations can be represented as

$$\mathcal{L}\mathbf{u} = \mathbf{g} \quad \text{in} \quad \Omega \quad (11)$$

$$\mathcal{B}\mathbf{u} = \mathbf{u}_\Gamma \quad \text{on} \quad \Gamma \quad (12)$$

with $\mathcal{L}$ a linear partial differential operator and $\mathcal{B}$ the trace operator.

For the present problem, the operator $\mathcal{L}_{\rm SP}$ for the single-phase regions is

$$\mathcal{L}_{SP} = \begin{Bmatrix} \dfrac{\partial}{\partial z} & 0 & 0 \\ \dfrac{\partial V^*}{\partial z} & \dfrac{\partial}{\partial z} & 0 \\ 0 & 0 & (\rho V)^* \dfrac{\partial}{\partial z} \end{Bmatrix} \quad (13)$$

and the unknowns vector $\mathbf{u}_{\rm SP}$ for the single-phase region is

$$\mathbf{u}_{SP} = \begin{bmatrix} \rho V & P & e \end{bmatrix} \quad (14)$$

For the two-phase region, the operator $\mathcal{L}_{\rm TP}$ is

$$\mathcal{L}_{\rm TP} = \begin{Bmatrix} \dfrac{\partial}{\partial z} & 0 & 0 \\ 0 & \dfrac{\partial}{\partial z} & 0 \\ V_{\rm v}^* \dfrac{\partial}{\partial z} + \dfrac{\partial V_{\rm v}^*}{\partial z} & V_{\rm l}^* \dfrac{\partial}{\partial z} + \dfrac{\partial V_{\rm l}^*}{\partial z} & \dfrac{\partial}{\partial z} \end{Bmatrix} \quad (15)$$

and the unknowns' vector $\mathbf{u}_{\rm TP}$ for the two-phase region are

$$\mathbf{u}_{\rm TP} = \begin{bmatrix} \alpha\rho_{\rm v}V_{\rm v} & (1-\alpha)\rho_{\rm l}V_{\rm l} & P \end{bmatrix} \quad (16)$$

The superscript asterisk means that this variable is a known value from the last iteration.

We assume that the system is well posed and the operator $(\mathcal{L}, \mathcal{B})$ is a continuous mapping between the function space $X(\Omega)$ onto the space $Y(\Omega) \times Y(\Gamma)$.

The norm equivalent functional becomes

$$\mathcal{J}(\mathbf{u}) \equiv \frac{1}{2} \parallel \mathcal{L}\mathbf{u} - \mathbf{g} \parallel^2_{Y(\Omega)} + \frac{1}{2} \parallel \mathcal{B}\mathbf{u} - \mathbf{u}_\Gamma \parallel^2_{Y(\Gamma)} \quad (17)$$

On the basis of variational analysis, the minimization statement is equivalent to

$$\lim_{\epsilon \to 0} \frac{d}{d\epsilon} \mathcal{J}(\mathbf{u} + \epsilon\, \mathbf{v}) = 0 \quad \forall\, \mathbf{u} \in X(\Omega) \quad (18)$$

Hence, the necessary condition for the minimization of $\mathcal{J}$ is equivalent to

Find $\mathbf{u} \in X(\Omega)$ such that

$$\mathcal{A}(\mathbf{u}, \mathbf{v}) = \mathcal{F}(\mathbf{v}) \quad \forall \mathbf{v} \in X(\Omega) \quad (19)$$

with

$$\mathcal{A}(\mathbf{u}, \mathbf{v}) = \langle \mathcal{L}\mathbf{u}, \mathcal{L}\mathbf{v} \rangle_{Y(\Omega)} + \langle \mathcal{B}\mathbf{u}, \mathcal{B}\mathbf{v} \rangle_{Y(\Gamma)} \quad (20)$$

$$\mathcal{F}(\mathbf{v}) = \langle \mathbf{g}, \mathcal{L}\mathbf{v} \rangle_{Y(\Omega)} + \langle \mathbf{u}_\Gamma, \mathcal{B}\mathbf{v} \rangle_{Y(\Gamma)} \quad (21)$$

where $\mathcal{A} : X \times X \to \mathbb{R}$ is a symmetric, continuous bilinear form, and $\mathcal{F} : X \to \mathbb{R}$ a continuous linear form.

The introduction of the boundary residual allows the use of spaces $X(\Omega)$ that are not constrained to satisfy the boundary conditions. The boundary terms can be omitted and the boundary conditions must be enforced strongly in the definition of the space $X(\Omega)$.

Finally, the searching space is restricted to a finite dimensional space such that $\mathbf{u}_h \in X_h(\Omega) \subset X(\Omega)$.

3.1 Spectral Element Approximation

The computational domain Ω is divided into N_e nonoverlapping subdomains Ω_e of diameter h_e, called spectral elements, such that

$$\Omega = \bigcup_{e=1}^{N_e} \Omega_e, \qquad \Omega_e \cap \Omega_l = \emptyset, \quad e \neq l \quad (22)$$

For reasons of efficiency, each subdomain is mapped onto the unit cube $[-1, 1]^d$, with $d = \dim \Omega$, by an invertible mapping.

In each element Ω_e the unknown function, $\mathbf{u}_h^e$, is approximated by $\mathbb{P}_{Q_e}$ (i.e., the set of all polynomials of degree $\leq Q_e$). The global approximation in Ω, $\mathbf{u}_h$, is constructed by gluing the local approximations $\mathbf{u}_h^e$, i.e.,

$$\mathbf{u}_h = \bigcup_{e=1}^{N_e} \mathbf{u}_h^e \tag{23}$$

Within each element, the solution is expanded in Φ_i continuous basis functions

$$\mathbf{u}_h^e(x,t) = \sum_{i=0} \mathbf{u}_i^e \Phi_i(\xi,\eta) \tag{24}$$

with $(\xi,\eta) = \chi_e^{-1}(x,t)$ the local coordinate of (x,t) in the parent element, with $-1 \leq \xi \leq 1$ and $-1 \leq \eta \leq 1$, and $\mathbf{u}_i^e$ the coefficients in the expansion.

4. SOLUTION ALGORITHM

In order to solve the system of equations (conservation of mass, momentum, and energy) showed in Section 2.1, we implemented a least-squares spectral element method. The one-dimensional domain is split into several slabs. We solve for only one element at a time and then use the solutions of the i_{th} slab as boundary conditions for the next slab (i+1). Some iterations are needed in order to achieve an acceptable error because of the nonlinearity of the system. As mentioned earlier a common representation for the understanding of two-phase flow instabilities is the plot of the total pressure drop along the heated section against the mass flow rate for a given heat flux. This representation is usually referred to as an "N-shape" curve because of the negative slope of the total pressure drop in the two-phase flow region. In this work, we used the model described in Section 2 to build the N-shape curves.

5. NECESSARY CONDITION FOR THE OCCURRENCE OF THE NEGATIVE SLOPE

We can state that the total pressure drop along the pipe is a function of the mass flux and the outlet quality (which is also a function of the mass flux), i.e., $\Delta P = \Delta P[G, x_{\text{out}}(G)]$. Then, if we are searching for the condition of a negative slope

$$\frac{d\Delta P}{dG} < 0 \tag{25}$$

with

$$\frac{d\Delta P}{dG} = \frac{\partial \Delta P}{\partial G} + \frac{\partial \Delta P}{\partial x_{\text{out}}} \frac{dx_{\text{out}}}{dG} \tag{26}$$

Because we want to find the negative slope in the plot within the mass fluxes where we have two-phase flow at the outlet, we can split the pressure drop into two terms, the pressure drop in the liquid region, and the term associated with the pressure drop in the two-phase flow region (this implies that our analysis is valid for the region between $0 \leq x_{\text{out}} \leq 1$)

$$\Delta P[G, x_{\text{out}}(G)] = \Delta P_{\text{l}}[G, x_{\text{out}}(G)] + \Delta P_{\text{tp}}[G, x_{\text{out}}(G)] \tag{27}$$

Finally, we can express the condition $(d\Delta P)/(dG) < 0$ as

$$\frac{\partial \Delta P_{\text{l}}}{\partial G} + \frac{\partial \Delta P_{\text{tp}}}{\partial G} < \left(\frac{\partial \Delta P_{\text{l}}}{\partial L_{\text{l}}} - \frac{\partial \Delta P_{\text{tp}}}{\partial L_{\text{tp}}} \right) \frac{\partial L_{\text{tp}}}{\partial x_{\text{out}}} \frac{dx_{\text{out}}}{dG} \tag{28}$$

where we always have

$$\frac{\partial \Delta P_{\text{l}}}{\partial G} > 0 \tag{29}$$

$$\frac{\partial \Delta P_{\text{tp}}}{\partial G} > 0 \tag{30}$$

$$\left(\frac{\partial \Delta P_{\text{l}}}{\partial L_{\text{l}}} - \frac{\partial \Delta P_{\text{tp}}}{\partial L_{\text{tp}}} \right) \leq 0 \tag{31}$$

$$\frac{\partial L_{\text{tp}}}{\partial x_{\text{out}}} \geq 0 \tag{32}$$

$$\frac{dx_{\text{out}}}{dG} \leq 0 \tag{33}$$

From Eq. (28), we should remark that, as it will be shown later, inequality (31) is very sensitive to the inlet pressure, while, inequality (32) is closely related with the heat distribution along the wall and (33) with the subcooling temperature.

6. NUMERICAL RESULTS

In the present section, we first analyze the behavior of the presure drop of a heated pipe as a function of the mass flux and then perform sensitivity analysis for several important parameters. The test conditions are 1010 kPa of inlet pressure, heat flux (defined with the outer diameter) of 11.9 kW/m^2, and 30 K of subcooling. The test fluid is R134a.

As can be seen in Fig. 2, the plot shows an N-shape behavior. This is because of the negative slope in the plot, which shows that in some region, the pressure drop gets higher as the flow rate goes down. This is due to the fact that, as the flow goes down, the change on the specific enthalpy of the fluid gets higher. Then, in the particular condition when the fluid at the outlet reaches the saturated conditions (flow rate ∼320 kg/m^{2}s in Fig. 3), as the flow rate slows down, a two-phase region starts to grow at the end of the pipe. Because the two-phase friction pressure drop is much larger than the liquid single-phase friction pressure drop, the net effect is a rising in the pressure drop.

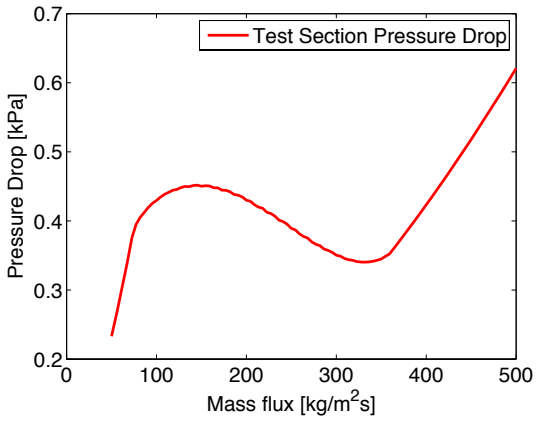

FIG. 2: Total pressure drop versus mass flow rate.

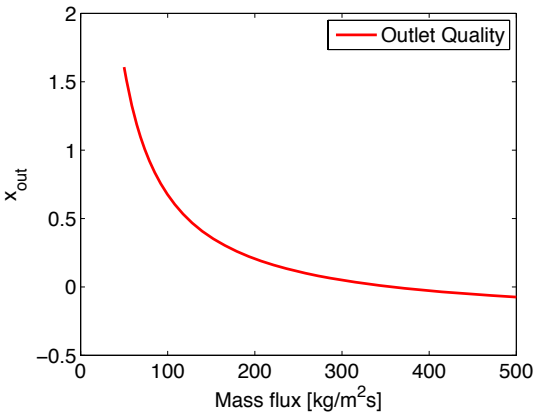

FIG. 3: Outlet quality versus mass flow rate.

6.1 Parameter Sensitivity Analysis

We are interested in the sensitivity of the response of the system to the variation of different parameters.

6.1.1 Effect of Inlet Pressure

First, we analyzed the effect of the inlet pressure. As the pressure gets higher, the densities and viscosities of the phases approaches each other. Then, the effect of the two-phase region in the pipe for the pressure drop gets lower. As can be seen in Fig. 4, as the working pressure gets higher, the N-shape gets flatter [higher inlet pressures stabilize the system as stated in Boure et al. (1973)]. We can see that the term inside the parentheses in the inequality (31) approaches zero as the pressure increases, making more difficult for Eq. (28) to be satisfied.

6.1.2 Effect of Inlet Temperature (Degree of Subcooling)

As Fig. 5 shows, the subcooling temperature plays a very important role in the slope of the pressure drop against the mass flow rate. This behavior agrees with the experimental results and steady-state model predictions from Kakac and Bon (2008) and Kakac and Cao (2009). As has been said before, the negative slope is due to the effect of a two-phase region that starts to grow from the outlet of the pipe. It can be seen from Eqs. (7) and (8) that for all the conditions fixed except the mass flux, we can always reach a mass flux at which the fluid is vapor at saturated conditions at the outlet [i.e., $L_{\mathrm{tp}} + L_{\mathrm{l}} = L$ (mass flux ∼80 kg/m^{2}s in Fig. 3]. From now on, we will refer to the

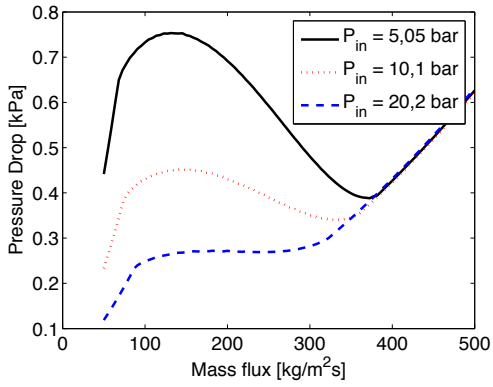

FIG. 4: Total pressure drop versus mass flux for different inlet pressures.

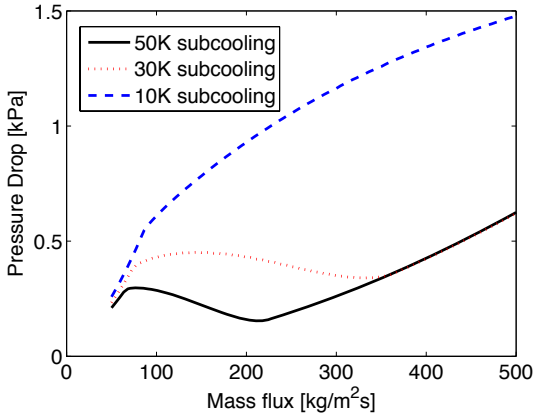

FIG. 5: Total pressure drop versus mass flux for different inlet subcooling temperatures.

particular mass flux where the outlet quality is equal to zero as G^*. Neglecting the kinetic term of the specific energy of the fluid, the lengths of the liquid and two-phase regions at this point ("characteristic lengths" from now on) will be (for a uniform heating profile)

$$L_{\mathrm{tp_{Ch}}} = L\frac{H_{\mathrm{lv}}}{H_{\mathrm{lv}} + c_{\mathrm{pl}}T_{\mathrm{sub}}} \tag{34}$$

$$L_{\mathrm{l_{Ch}}} = L\frac{c_{\mathrm{pL}}T_{\mathrm{sub}}}{H_{\mathrm{lv}} + c_{\mathrm{pl}}T_{\mathrm{sub}}} = \frac{1}{H_{\mathrm{lv}}/(c_{\mathrm{pl}}T_{\mathrm{sub}}) + 1}L \tag{35}$$

where L is the total length of the heated section, and $L_{\mathrm{tp_{Ch}}}$ and $L_{\mathrm{l_{Ch}}}$ are the two-phase and liquid characteristic lengths respectively. It can be seen from Eq. (35) that the larger the subcooling temperature gets, the larger the liquid characteristic length gets. This fact can make us think that because a larger subcooling leads to a smaller two-phase flow charactertistic length, it is expectable that the N-shape gets flatter as we increase the subcooling temperature (Fig. 5 shows the opposite trend). But there is another factor that must be taken into account, which is the growth rate of this two-phase region as a function of a given variation in the mass flux, (i.e., $(\partial L_{\mathrm{tp}})/(\partial G)$). As can be seen in Fig. 3, the outlet quality has a hyperbolic trend as a function of the mass flow rate (independent of the heat flux profile, as long as it remains constant for the different mass fluxes). The relation between the quality of the fluid at the outlet of the pipe and the mass flux can be expressed as

$$x_{\mathrm{out}} = \frac{1}{G}\frac{qL\mathrm{Per}}{AH_{\mathrm{lv}}} - \frac{c_{\mathrm{pl}}T_{\mathrm{sub}}}{H_{\mathrm{lv}}}, \tag{36}$$

where x_{out} is the thermodynamic quality at the outlet, Per is the heated perimeter and A is the cross section area of the pipe. We can see from Eq. (36) that as G goes to infinity, x_{out} goes to $-c_{\mathrm{pl}}T_{\mathrm{sub}}/H_{\mathrm{lv}}$. Thus, for subcooling temperatures close to zero, the quality at the outlet reaches zero for mass fluxes extremely large, as is expected. But what is important, is that the slope of the outlet quality as a function of the mass flux is close to zero when the outlet quality approaches the zero value (this effect can be observed in Fig. 6). This slope gives an idea of the amount of change in the outlet quality for a given change in the mass flux. The quality at the outlet is related with the length of the two-phase region. This means that for outlet quality equal to zero, the two-phase region length is zero, and for outlet quality equal to 1, the length of the two-phase region reaches its maximun value. Thus, the slope of the outlet quality at $G = G^*$ somehow shows the rate of growth of the two-phase region length as a function of the decrease in the mass flux (actually, the two-phase flow length grows linearly with the decrease in the mass flux for uniform heating). If we take a look at Eq. (28), then we can see how the term related with the subcooling [inequality (33)] brings the right-hand side of Eq. (28) to zero (i.e., no N-shape in the plot).

Thus, all this means that while larger subcooling implies, in principle, longer liquid characteristic lengths, this effect can be overcome by the rate of growth of the outlet quality with changes in the mass flux, thus resulting in a

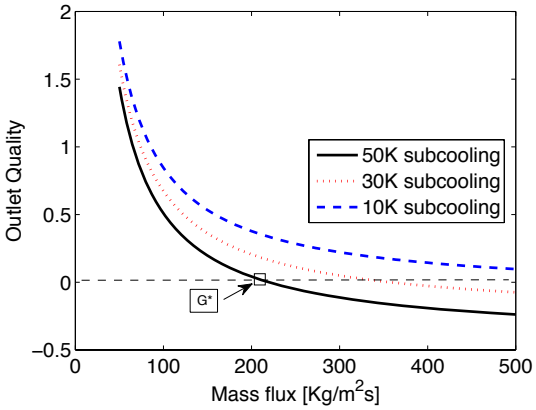

FIG. 6: Outlet quality versus mass flux for different inlet subcooling temperatures.

sudden increase in the pressure drop with the decrease in the mass flux for outlet qualities close to zero.

In order to show the behavior of the system as a function of the degree of subcooling, the slope of the outlet quality with respect to the mass flux at G^* as a function of the subcooling is plotted in Fig. 7.

6.1.3 *Effect of Heating Power*

In order to know if the amount of heat applied to the fluid has any influence on the shape of the pressure drop plot, we perform several simulations with different uniform heating powers. The results are shown in Fig. 8. More heat

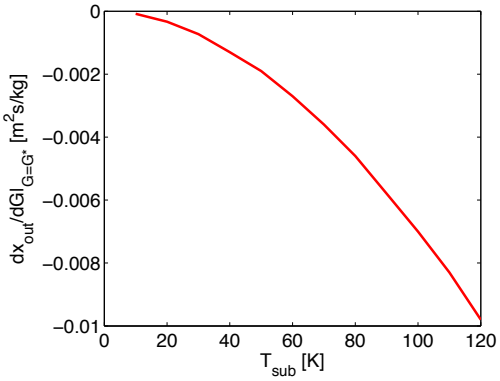

FIG. 7: Slope of the outlet quality with respect to the mass flux at $G = G^*$ versus subcooling temperature.

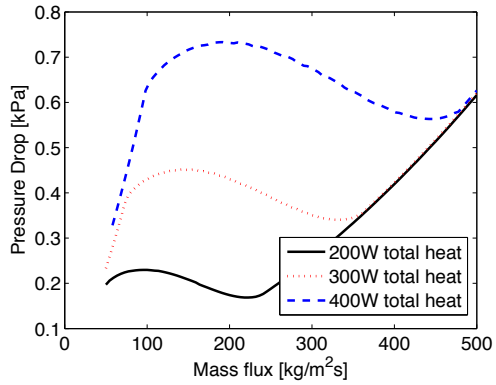

FIG. 8: Total pressure drop versus mass flux for different total heating power.

applied to the fluid implies that for the same flow rate, the enthalpy at the outlet will be higher. However, because we are interested in the shape of the plot, the relative values and not the absolute ones are the important. Thus, as can be seen from Fig. 8, if we, for example, decrease the amount of heat applied to the fluid, but also decrease the mass flux range in the same proportion, the shape of the N-shape curve will be the same.

Note that this analysis has been done with an horizontal pipe. On the other hand, in vertical pipes, the N-shape changes its shape when the heating power is increased or reduced. In this case, the gravitational component of the pressure drop has a stabilizing effect for upward boiling configuration, while it has a destabilizing effect for downward flow boiling configurations (see Babelli and Ishii, 2001; Kakac and Cao, 2009; Kakac and Liu, 1991; Kakac et al., 1990; Wang et al., 1996). The increasing of heating power and mass flow rates, in both cases, lowered the relative effect of the gravitational component of the pressure drop (independent of the mass flow rate).

It should be also noted that this model does not take into account the subcooled boiling phenomena, which can play a significant role in the pressure drop for high heat fluxes and low outlet qualities (Cao et al., 2000).

6.1.4 *Effect of Heating Power Distribution*

As previously mentioned, the amount of heat applied to the fluid has no influence on the relative slope of the pressure drop versus mass flux plot. However, there is one more effect on the heating that must be taken into account. This effect is the distribution of the heat applied along the pipe. As we know, for the case of heat exchangers, the heat exchanged between the fluids is proportional to the temperature difference (together with other important parameters), which will give a nonuniform heat flux profile. In this analysis, for simplicity, we observe the effect of linear, quadratic, and cubic profiles. All the profiles have the same mean value, both starting from zero at the inlet, or ending at the outlet of the pipe with zero heat flux.

Figure 9 shows the effect of the different heating distributions on the pressure drop versus mass flux plot with all the nonuniform profiles starting from zero and growing monotonously until the end of the heating section. It should be remarked that the mean value of all the heat flux distributions is the same. The different heat flux profiles are plotted in Fig. 10. It can be seen that as more of the heat is applied at the end of the heated section, the N-shape plot gets flatter. On the other hand, Fig. 11 shows the effect of the different heating distributions on the pres-

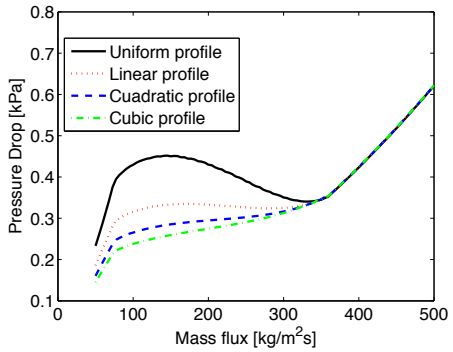

FIG. 9: Total pressure drop versus mass flux for monotonically increasing heating power profiles.

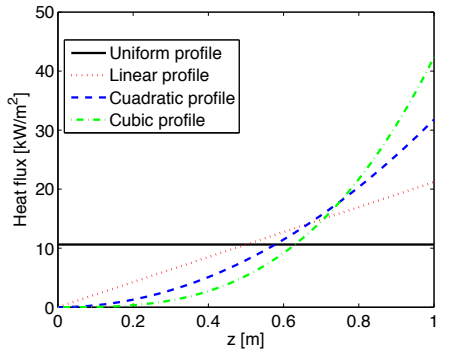

FIG. 10: Different monotonically increasing heating power profiles applied along the heated pipe.

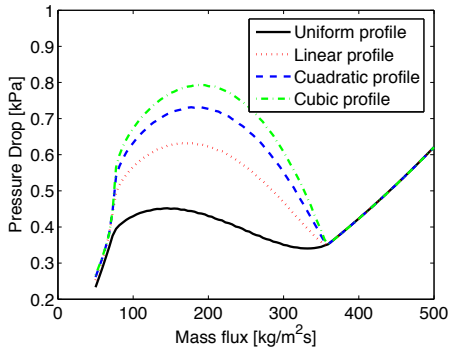

FIG. 11: Total pressure drop versus mass flux for monotonically decreasing heating power profiles.

sure drop versus mass flux plot with all the nonuniform profiles starting from its maximum value and decreasing monotonously until zero at the end of the heating section. In Fig. 12, we can see the different heat flux profiles for this case. The results obtained in Fig. 11 confirm that if most of the heat flux is applied at the beginning of the heated section (actually the typical case in heat exchangers), the negative slope in the N-shape plot gets steeper.

As previously mentioned, the rate of growing of the two-phase region length as a function of the mass flux is an important factor for the presence of a negative slope in the pressure drop versus mass flux plot. We have analyzed before the relation between the outlet quality and the mass flux and found that it is closely related to the subcooling temperature and independent of the heat distribution. Now we will analyze the relation between the two-phase region length and the outlet quality, which is strongly influenced by the heating profile distribution. If we neglect the kinetic energy term of the specific energy of the fluid, then we can express the two-phase region length as a function of the outlet quality as

$$L_{\rm tp} = L - Q^{-1}\left[qL\frac{(c_{\rm pl}T_{\rm sub})/H_{\rm lv}}{x_{\rm out}-(c_{\rm pl}T_{\rm sub})/H_{\rm lv}} - Q(z_{\rm o})\right], \quad (37)$$

where Q is the primitive function of the heat flux q_w, the superscript -1 means the inverse of the function, $x_{\rm out}$ the outlet quality, and $z_{\rm o}$ is the axial coordinate at the beginning of the heated section.

For the case of uniform heat flux $q_{\rm w}$ applied to the wall, Eq. (37) becomes

$$L_{\rm tp} = L\left\{1 - \left[\frac{(c_{\rm pl}T_{\rm sub})/H_{\rm lv}}{x_{\rm out}+(c_{\rm pl}T_{\rm sub})/H_{\rm lv}}\right]\right\} \quad (38)$$

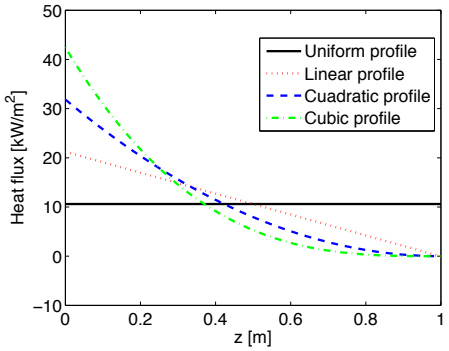

FIG. 12: Different monotonically decreasing heating power profiles applied along the heated pipe.

and the partial derivative with respect to the outlet quality

$$\frac{\partial L_{\rm tp}}{\partial x_{\rm out}} = L\frac{(c_{\rm pl}T_{\rm sub})/H_{\rm lv}}{\left[x_{\rm out}+(c_{\rm pl}T_{\rm sub})/H_{\rm lv}\right]^2} \tag{39}$$

If we solve Eq. (37) for the case of a monotonically increasing linear heating power profile, then we get for $L_{\rm tp}$:

$$L_{\rm tp} = L\left\{1-\left[\frac{(c_{pl}T_{\rm sub})/H_{\rm lv}}{x_{\rm out}+(c_{\rm pl}T_{\rm sub})/H_{\rm lv}}\right]^{1/2}\right\} \tag{40}$$

The partial derivative with respect to the outlet quality for this case becomes

$$\frac{\partial L_{\rm tp}}{\partial x_{\rm out}} = \frac{L}{2}\frac{\left[x_{\rm out}+(c_{\rm pl}T_{\rm sub})/H_{\rm lv}\right]^{3/2}}{\left[(c_{\rm pl}T_{\rm sub})/H_{\rm lv}\right]^3} \tag{41}$$

Solving Eq. (37) for the case of a monotonically decreasing linear heating power profile, we get for the two-phase flow length

$$L_{\rm tp} = L\left\{1-\left[\frac{(c_{\rm pl}T_{\rm sub})/H_{\rm lv}}{x_{\rm out}+(c_{\rm pl}T_{\rm sub})/H_{\rm lv}}\right]\right\}^{1/2} \tag{42}$$

and the partial derivative with respect to the outlet quality becomes

$$\frac{\partial L_{\rm tp}}{\partial x_{\rm out}} = \frac{L}{2}\frac{(c_{\rm pl}T_{\rm sub})/H_{\rm lv}}{x_{\rm out}^{1/2}\left(x_{\rm out}+(c_{\rm pl}T_{\rm sub})/H_{\rm lv}\right)^{3/2}}. \tag{43}$$

Equations (39), (41) and (43) show the form of the term of inequality (32) for different heating profiles configurations. It should be noted that this term is independent of the mean value of the heating power. This term acts like a "tunner" in Eq. (28). This means that, if for example, the inlet pressure is high [term of Eq. (31) goes down] and the subcooling temperature is small [term of Eq. (33) goes down], then it could still be possible to reach the necessary condition for the ocurrence of the negative slope [Eq. (28)]. The opposite is also true, i.e., even with a big subcooling and low pressure at the inlet of the pipe, it could be possible to avoid the presence of a negative slope with a given heat flux profile distribution. For example, Eq. (43) goes to infinity as the outlet quality goes to zero, which agrees with the influence of the linear decreasing heating profile in the N-shape plot.

Another important fact is that the heating profile along the pipe wall also modifies the liquid and two-phase characteristic lengths [Eqs. (34) and (35) are not valid any more]. For the case where most of the heat is concentrated at the beginning, the two-phase characteristic length is much longer (and the liquid charecteristic length is much shorter) than for the case where the most of the heat is applied at the end.

7. CONCLUSIONS

The pressure drop along a heated pipe with subcooled liquid at the inlet as a function of the mass flux has been modeled in this work. This behavior, usually referred to as N-shape plot, can present a negative slope in the region when the fluid at the outlet is in boiling conditions (two-phase flow). This negative slope, which is the main responsible for the occurrence of pressure drop and thermal instabilities, is not always present and it depends on several factors. It was found that the working pressure is a very important factor in the behavior of the fluid, observing that for higher inlet pressures the negative slope gets less steep. This is due to the fact that as we get closer to the critical pressure of the fluid, the difference between the vapor and the fluid densities and viscocities gets lower. Another effect that plays an important role in this plot is the inlet temperature. It was found that the negative slope was steeper for larger subcoolings. This behavior can be explained observing the evolution of the outlet quality as a function of the mass flux. As the inlet temperature approaches the saturation temperature at the inlet pressure, the slope of the outlet quality as a function of the mass flux gets closer to zero. This means that for higher subcoolings the change in the outlet quality for a given mass flux variation will be larger, and the outlet quality is closely related with two-phase region length inside the pipe, with a final effect of a domination in the total pressure pressure drop by the two-phase region length over the mass flux. No significant effect was found in the heating power (the relative shape of the plot remains the same), but the distribution of the heat along the pipe was found to be a key factor. If most of the heat is applied at the inlet of the pipe, then when we decrease the mass flux from the point where the fluid is saturated liquid at the outlet, the two phase region will grow much faster than if most of the heat is concentrated at the end of the heated section.

ACKNOWLEDGEMENTS

The Ph.D. fellowship (E. M. C.) financed by the NTNU-SINTEF Gas Technology Centre through the Two Phase Flow Instabilities project is gratefully appreciated.

REFERENCES

Babelli, I. and Ishii, I., Flow excursion instability in downward flow systems part II: Two-phase instability, *Nucl. Eng. Des.*, vol. **206**, pp. 97–104, 2001.

Boure, J., Bergles, A., and Tong, L., Review of two-phase flow instabilities, *Nucl. Eng. Des.*, vol. **25**, pp. 165–192, 1973.

Cao, L., Kakac, S., Liu, H., and Sarma, P., The effects of thermal non-equilibrium and inlet temperature on two-phase flow pressure drop type instabilities in an upflow boiling system, *Int. J. Thermal Sci.*, vol. **39**, pp. 886–895, 2000.

Farhadi, K., A model for predicting static instability in two-phase flow systems, *Prog. Nucl. Energy*, vol. **51**, pp. 805–812, 2009.

Gungor, K. and Winterton, R., Simplified general correlation for saturated flow boiling and comparisons of correlations with data, *Chem. Eng. Res. Des.*, vol. **65**, pp. 148–156, 1987.

Gurgenci, H., Veziroglu, T., and Kakac, S., Symplified nonlinear descriptions of two-phase flow instabilities in vertical boiling channel, *Int. J. Heat Mass Transfer*, vol. **26**, pp. 671–679, 1983.

Haaland, S., Simple and explicit formulas for the skin friction in turbulent pipe flow, *J. Fluids Eng.*, vol. **105**, pp. 89–90, 1983.

Jiang, B., *The Least-Square Finite Element Method: Theory and Applications in Computational Fluid Dynamics and Electromagnetics*, Springer, New York, 1998.

Kakac, S. and Bon, B., A review of two-phase flow dynamic instabilities in tube boiling systems, *Int. J. Heat Mass Transfer*, vol. **51**, pp. 399–433, 2008.

Kakac, S. and Cao, L., Analysis of convective two-phase flow instabilities in vertical and horizontal in-tube boiling systems, *Int. J. Heat Mass Transfer*, vol. **52**, pp. 3984–3993, 2009.

Kakac, S. and Liu, H., An experimental investigation of thermally induced flow instabilities in a convective boiling upflow system, *Warme- Stoffbertrag.*, vol. **26**, pp. 365–376, 1991.

Kakac, S., Veziroglu, T., Padki, M., Fu, L., and Chen, X., Investigation of thermal instabilities in a forced convection upward boiling system, *Exp. Thermal Fluid Sci.*, vol. **3**, pp. 191–201, 1990.

Liu, H., Kocak, H., and Kakac, S., Dynamical analysis of pressure-drop type oscillations with a planar model, *Int. J. Multiphase Flow*, vol. **21**, pp. 851–859, 1995.

Sripattrapan, W. and Wongwises, S., Two-phase flow of refrigerants during evaporation under constant heat flux in a horizontal tube, *Int. Commun. Heat Mass Transfer*, vol. **32**, pp. 386–402, 2005.

Stephan, K., *Heat Transfer in Condensation and Boiling*, Springer-Verlag, Berlin, 1992.

Wang, Q., Chen, X., Kakac, S., and Ding, Y., Boiling onset oscillation: A new type of dynamic instability in a forced-convection upflow boiling system, *Int. J. Heat Fluid Flow*, vol. **17**, pp. 418–423, 1996.

Whalley, P., *Boiling, Condensation, and Gas-Liquid Flow*, Clarendon Press, Oxford, 1987.